DOI: 10.1007/s10967-007-0412-x Journal of Radioanalytical and Nuclear Chemistry, Vol. 276, No.1 (2008) 71–77

Prompt-gamma neutron activation analysis system design: Effects of D-T versus D-D neutron generator source selection

R. J. Shypailo,* K. J. Ellis

USDA/ARS Children's Nutrition Research Center, Department of Pediatrics, Baylor College of Medicine, Houston, TX 77030, USA

(Received January 3, 2007)

Prompt-gamma neutron activation (PGNA) analysis is used for the non-invasive measurement of human body composition. Advancements in portable, compact neutron generator design have made those devices attractive as neutron sources. Two distinct generators are available: D-D with 2.5 MeV and D-T with 14.2 MeV neutrons. To compare the performance of these two units in our present PGNA system, we performed Monte Carlo simulations (MCNP-5; Los Alamos National Laboratory) evaluating the nitrogen reactions produced in tissue-equivalent phantoms and the effects of background interference on the gamma-detectors. Monte Carlo response curves showed increased gamma production per unit dose when using the D-D generator, suggesting that it is the more suitable choice for smaller sized subjects. The increased penetration by higher energy neutrons produced by the D-T generator supports its utility when examining larger, especially obese, subjects. A clinical PGNA analysis design incorporating both neutron generator options may be the best choice for a system required to measure a wide range of subject phenotypes.

Introduction

The prompt-gamma neutron activation (PGNA) system at the Children's Nutrition Research Center (CNRC) is designed to measure total body nitrogen (TBN) in vivo.[1] Similar PGNA systems have proven to be useful, both clinically and in research settings, for assessment of TBN,[2–4] a direct measure of total body protein (TBP), a major component of lean body mass.[5]

The present CNRC system was designed to minimize calibration difficulties due to non-linear particle efficiency and background interference commonly associated with PGNA systems.[3,6,7] Much of the design work was accomplished utilizing the modeling capabilities of the MCNP Monte Carlo program (Los Alamos National Laboratory).[8] Evaluations included neutron source positioning, shielding construction, and detector placement to obtain signal uniformity and maximum counting sensitivity per unit dose. The system uses a D-T neutron generator (MF Physics, Model A-325) which produces 14 MeV neutrons at a maximum yield of $1 \cdot 10^9$ n/s.

The present CNRC system for measuring TBN makes use of the 10.8 MeV gamma-rays produced by the thermal $^{14}N(n,\gamma)^{15}N$ reaction.[1] Its predecessor utilized an isotopic $^{241}AmBe$ neutron source (15.5 Ci) having a lower mean neutron energy of about 5 MeV.[9] These differences in neutron energies will result in variations in thermal activation depth, gamma signal uniformity, and overall counting efficiencies.[10,11]

We have recently obtained a D-D neutron generator (MF Physics, Model A-325DD) that has similar physical characteristics to the D-T unit, but produces less energetic neutrons (2.5 MeV) at a lower rate ($\sim 1 \cdot 10^7$ n/s). The energy of this generator is close to that of ^{252}Cf, a common neutron source for in vivo PGNA.[12,13] We wished to evaluate the potential advantages of using this D-D generator in the existing CNRC counting system for TBN measurement.

We wanted to minimize the redesign of the CNRC irradiator, which was achievable since the D-D neutron generator shares the same physical characteristics as the D-T generator. We intended to use the capabilities of the MCNP modeling program to examine the effect the D-D generator would have on the measurement of TBN. The program would allow us to virtually compare the D-T and D-D generator performances, including the effect of repositioning the "new" neutron source on system response. The Monte Carlo modeling approach had aided us previously in finalizing the CNRC design. We are now expanding on those efforts by evaluating different neutron source options within the present CNRC design parameters, without a significant redesign of the current irradiator/detector/shielding system.

Experimental

The physical design of the existing CNRC prompt-gamma irradiator was used as the basis for the Monte Carlo model. Materials defined in the model were based on the actual materials used in the irradiator. The size and composition of the neutron shield block and source collimator, the position of the patient bed, and the use of shielded detectors were all simulated. The major structural components used in the Monte Carlo runs are shown in Fig. 1. The detectors were defined as Bismuth-Germanate (BGO) crystals having a density of 7.1 g/cm^3. The neutron source was represented by a small steel sphere 2 cm in diameter, and could be repositioned in the model as needed to test various options for source configuration. This latest Monte Carlo model was similar to that described previously, with the exception of the added shielding surrounding the detectors.[1]

* E-mail: shypailo@bcm.edu

0236–5731/USD 20.00

Akadémiai Kiadó, Budapest
Springer, Dordrecht

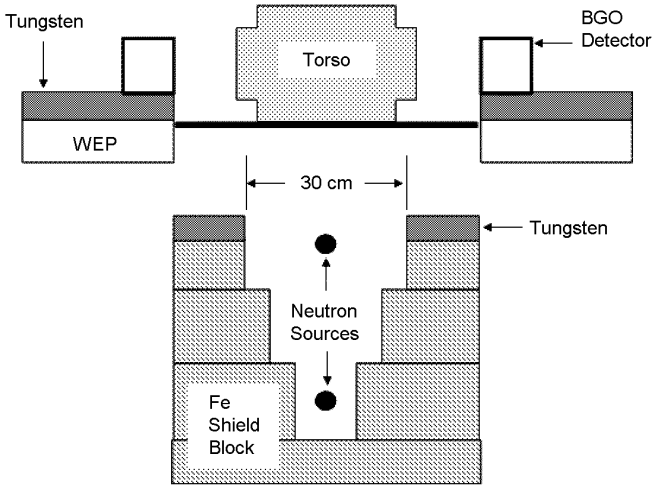

Fig. 1. Basic components of the CNRC prompt-gamma irradiator, as modeled within the MCNP program. Two optional source positions are depicted

The representation of the human torso on the bed was defined by a series of blocks filled with tissue-equivalent concentrations of carbon, oxygen, hydrogen, and nitrogen. The cross sectional dimensions were based on axial CT slices obtained for adults of average size (Fig. 2). A portion of each torso object was comprised of an array of discrete cube-shaped cells measuring 4 cm per side. The remaining torso was represented by larger cells. Only part of the torso was subdivided into the small cubes in order to simplify the model and reduce processing time. The model's response to particle scattering and interaction was considered to be bilaterally symmetrical, thus there was no need to always meticulously simulate both halves of the torso. A smaller torso was also constructed in a similar manner, based on an average-sized child 10-yr of age.

The neutron source was defined as either D-T (14.2 MeV, $1 \cdot 10^9$ n/s) or D-D (2.45 MeV, $1 \cdot 10^7$ n/s) in order to simulate the output of the two generators. The generators are physically interchangeable. Both units can be connected to the same high voltage power supply and operated by the same control console. Because the neutron yield from the D-D generator was 100 times smaller than that of the D-T generator, a set of simulations was run with the D-D unit positioned towards the top of the collimator, 25 cm from the torso surface. This was done to compensate for the lower neutron production by the D-D generator.

The MCNP runs were constructed to compare the effect of the two different neutron sources on the counting system. Neutron flux tallies, monitoring radiative capture within the adult-sized torso, were used to estimate gamma signal production uniformity and efficiency. These tallies focused on the individual cubic cells of the torso, thus both lateral and depth-dependant flux distribution could be obtained. Since the final system is to be used in pediatric clinical populations, similar neutron flux tallies were also run for a smaller sized torso.

Energy deposition tallies provided estimates of absorbed dose to the torso, and also monitored areas further removed from the target area that is directly above the collimator. These tallies involved cells along the torso surface in the longitudinal direction (i.e., the axis of the bed), in order to estimate absorbed dose away from the collimator area.

Pulse-height tallies were used to estimate gamma signal response within the detectors. This final set of tallies was run in NP (neutron-photon) mode and was used to quantify the photons entering the detectors that had been produced by neutron activation. Most simulations processed at least $5 \cdot 10^6$ particle histories, resulting in relative errors ranging from 0.01 to 0.08. Mixed mode (i.e., neutron/photon) runs, used to assess pulse height in detector cells, required longer processing times. Those simulations required at least $6 \cdot 10^7$ particle histories in order to achieve relative errors of less than 0.10, and ran for up to 14 hours. MCNP tallies should have relative errors of less than 0.10 in order to produce generally reliable results.

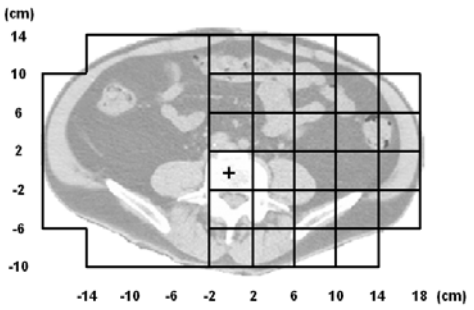

Fig. 2. Cross sectional view of torso partially divided into 4 cm×4 cm cells

Variance reduction techniques, such as source biasing, were not used in these MCNP runs. Particles were allowed to scatter in all directions. Since we were evaluating overall system response to different neutron sources, and since particle interaction with system components affects the final response in a PGNA system, allowing the sources to behave normally should produce more realistic tally estimates.

Results

Neutron flux tally results for gamma production via radiative capture (n,γ) for each neutron generator are presented in Fig. 3. Both generators were identically positioned within the collimator, about 60 cm from the torso surface. Target torso cells were 4 cm from the surface. The tallies represent the cross-sectional region directly above the collimator. As expected the D-D generator exhibited greater nitrogen gamma production per source neutron than the D-T generator. For the center 20 cm region, production from the D-D was about 22% higher. Both generators showed similar lateral flux distribution patterns – fairly uniform throughout the middle 15–20 cm of the torso, with a decrease in flux toward the outer edges.

Gamma production tallies were run comparing the D-T generator at its normal position with the D-D generator moved closer to the torso (distance = 25 cm). Tables 1 and 2 show the relative distribution of gammas produced throughout the torso for each case, for a single axial slice directly above the collimator. Gamma production is highest at a 4 cm depth from the torso surface. The D-D generator shows greater production within the torso, relative to the surface torso cells, than the D-T. For example, at lateral position 0, D-D generator gamma production increases by 37% at a depth of 4 cm, then drops to a value close to unity at an 8 cm depth. In contrast, the D-T generator showed an increase of about 31% at 4 cm, and then decreased to 80% of the initial surface value at the 8 cm depth.

Pulse pileup is a significant source of interference for PGNA analysis. Gamma production due to neutron collisions within the detectors and torso was evaluated for each generator and for the two torso sizes (Table 3). The values represent average gamma production within the detectors and torso cells. A signal to noise ratio, defined as the torso signal divided by the detector signal, is also calculated. Overall, gamma production was higher for the D-D generator. The change in gamma production is similar when comparing an adult torso with a pediatric torso for both generators, but the activity in the detector cells decreases substantially in pediatric mode (–77.4% vs. –14.5%), indicating an improvement in signal to noise ratio for the D-D generator with the pediatric torso: 0.12 vis-à-vis 0.03 for the D-T generator.

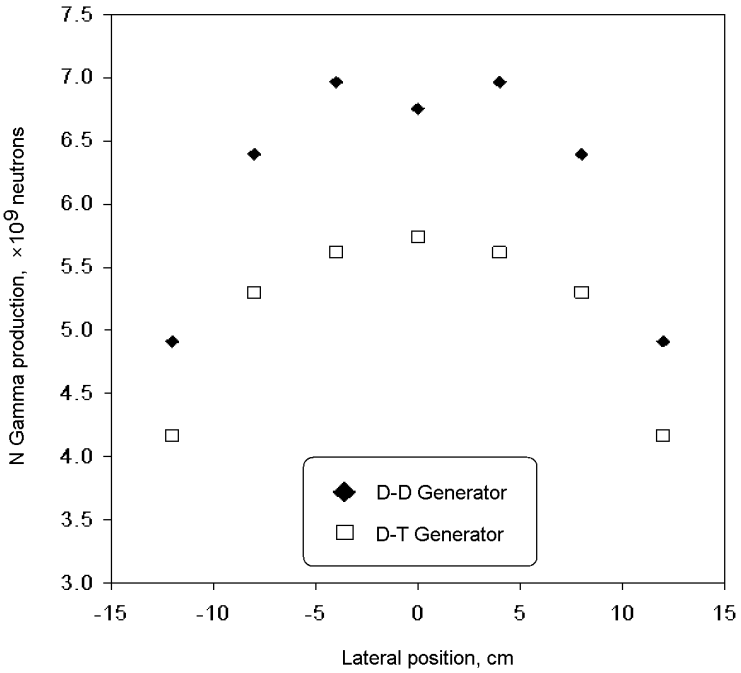

Fig. 3. Radiative capture gamma production within the torso at a 4 cm depth

Table 1. Nitrogen gamma production* in torso cells using D-D neutron generator

Depth, cm	Lateral position, cm								
	–16	–12	–8	–4	0	4	8	12	16
0	**	0.60	0.89	0.96	1.00	0.96	0.89	0.60	**
4	0.45	0.97	1.25	1.34	1.37	1.34	1.25	0.97	0.45
8	0.44	0.80	0.92	0.97	0.98	0.97	0.92	0.80	0.44
12	0.28	0.48	0.53	0.56	0.56	0.56	0.53	0.48	0.28
16	0.12	0.24	0.28	0.28	0.28	0.28	0.28	0.24	0.12
20	**	0.07	0.10	0.10	0.10	0.10	0.10	0.07	**

* Values represent gamma production relative to surface torso cell directly above collimator.
** Positions not tallied; not part of torso.

Table 2. Nitrogen gamma production* in torso cells using D-T neutron generator

Depth, cm	Lateral position, cm								
	–16	–12	–8	–4	0	4	8	12	16
0	**	0.63	0.92	1.00	1.00	1.00	0.92	0.63	**
4	0.44	0.95	1.21	1.28	1.31	1.28	1.21	0.95	0.44
8	0.40	0.68	0.77	0.77	0.80	0.77	0.77	0.68	0.40
12	0.24	0.40	0.42	0.43	0.39	0.43	0.42	0.40	0.24
16	0.10	0.13	0.22	0.19	0.20	0.19	0.22	0.13	0.10
20	**	0.05	0.08	0.07	0.07	0.07	0.08	0.05	**

* Values represent gamma production relative to surface torso cell directly above collimator.
** Positions not tallied; not part of torso.

Table 3. Effect of torso size on relative nitrogen gamma production*

Site	D-D generator			D-T generator		
	Adult	Pediatric	Delta**	Adult	Pediatric	Delta**
Torso (signal)	8.51E-09	9.31E-09	9.3%	2.38E-09	2.70E-09	13.2%
Detector (bkd)	3.41E-07	7.71E-08	–77.4%	9.52E-08	8.14E-08	–14.5%
S/N Ratio	0.02	0.12		0.03	0.03	

* Values represent average N gamma production per starting particle.
** Percent change in gamma production for pediatric-size torso vs. adult-size torso.

Signal production is also slightly more uniform with the D-D generator. Uniformity was defined as:

$$U = \frac{S_{max} - S_{min}}{S_{max} + S_{min}} \times 100\%$$

where S_{max} and S_{min} are maximum and minimum signal values in an array.[14] Uniformity indices for the entire torso array are 90.4% and 92.9% for the D-D and D-T simulations respectively. Calculating the uniformity index for only the first three rows of cells (i.e., the lower half of the cell array), an area showing the greatest gamma production, indices improve to 51.3% and 53.5%. The D-D generator displays better uniformity of gamma signal production, but the two generators differ by only about 2%.

For MCNP runs designed to assess potential dose to the subject, the D-D generator was placed 25 cm below the torso surface, while the D-T generator remained 60 cm away. Energy deposition tallies with appropriate conversion multipliers yielded results in rads. Tally results (given per starting particle) were then adjusted for the average neutron generator output and for a hypothetical 3600-second scan time. The calculated entrance dose, in mSv, is given for torso surface cells along both lateral and longitudinal axes (Figs 4 and 5).

In the longitudinal direction, the two simulations show differences in dose distribution. The D-D generator shows a dose decrease of about 24% at a distance of 16 cm away from the collimator center. Estimated dose from the D-T generator drops by about 77% at these same distances, due mainly to source collimation.

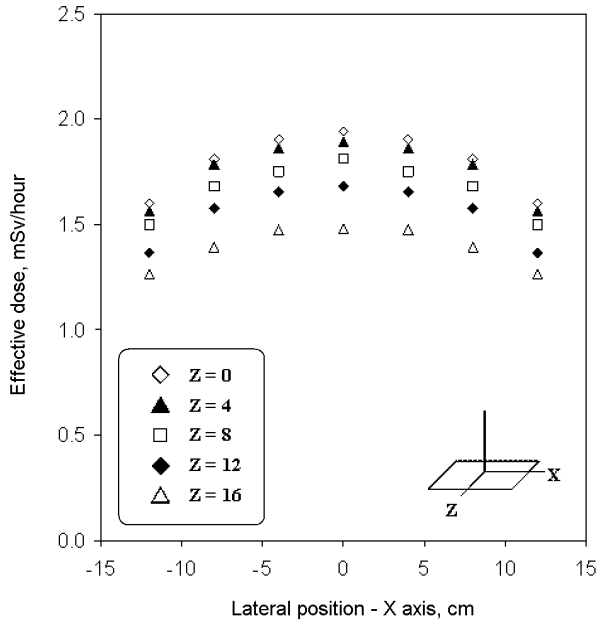

Fig. 4. Torso dose distribution in two dimensions from the D-D generator neutron source. Z indicates longitudinal position

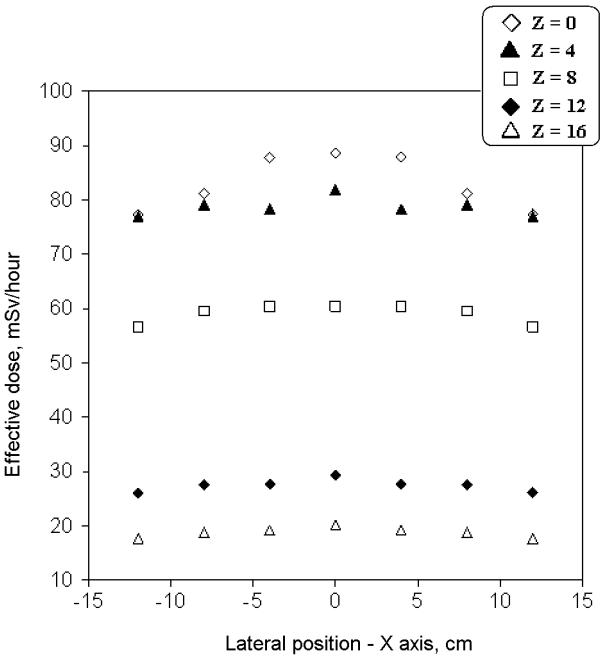

Fig. 5. Torso dose distribution in two dimensions from the D-T generator neutron source. Z indicates longitudinal position

The effect of the two neutron sources on detector response was investigated using pulse height tallies targeting detector cells. The runs produced energy distribution spectra of pulses created within the detectors. The principal element of interest was nitrogen, thus only the higher-energy portions of the resulting spectra are shown in Fig. 6. Both detectors show a distinct peak at 10.8 MeV that is attributed to the thermal $^{14}N(n,\gamma)^{15}N$ reaction. The D-T generator also produces sizable Fe peaks at about 8.8 and 8.3 MeV, as well as other smaller peaks in the spectral continuum. The simulated spectrum produced by the D-D generator does not exhibit as many of these smaller peaks in its background continuum, and the Fe peak is not present.

A direct comparison of the estimated number of pulses created in the detector cells for the existing neutron generators can be seen in Fig. 6. In determining the estimated counts for these spectra, the pulses per starting particle were multiplied by the neutron yield for each generator (neutrons/second), then by an estimated count time of 1000 seconds. The D-T generator spectrum shows a much higher nitrogen peak, exceeding the peak from the D-D spectrum by two orders of magnitude. The larger nitrogen peak associated with the D-T generator is due to that unit's greater neutron output. On a per neutron basis, the initial pulse height tally result for the detectors is actually higher for the D-D generator, $5.0 \cdot 10^{-6}$ vs. $1.5 \cdot 10^{-6}$ pulses per starting source particle.

Discussion

The potential advantage of using a lower energy neutron source, such as the D-D generator (2.45 MeV) is greater signal production per unit dose.[12,15] Gamma production tallies presented in Fig. 3 confirm this advantage.

Nitrogen gamma production uniformity is comparable for the two generators, even when positioning the D-D generator much closer to the torso (25 cm vs. 60 cm) (Tables 1 and 2). If bilateral irradiation was used during subject scanning, with both a prone and supine scan used to generate the final result, signal uniformity would improve to nearly 50% for the entire torso slice for both generators. Thus, the closer proximity of the D-D generator to the torso does not seem to have a significant negative effect on signal uniformity.

Bringing the D-D generator closer to the torso surface would increase the dose rate to the subject, thus the effect of this approach was examined in the dose profile curves (Figs 4 and 5). The D-T generator remained positioned well within the collimator, while the D-D generator was raised to the top of the collimator. Without additional shielding, the D-D generator would potentially expose a larger area of the torso to unnecessary dose, since the counting region of interest lies directly above the collimator. This was confirmed by the smaller decrease in dose to adjacent areas when using the D-D generator. Nevertheless, absolute doses from the current D-D generator are much lower than those from the D-T generator, which showed an average absorbed dose about thirty times higher than

the D-D. This is predominately attributable to the much higher neutron output of the D-T generator.

It should be noted that the Monte Carlo simulations that were performed using MCNP do not fully account for the neutron effects on the performance of the detectors and associated electronics. The high count rates associated with PGNA systems and resulting pileup within the detectors are known problems. Most pileup events are due to the large number of lower energy signals entering the detectors. According to MCNEILL et al.,[15] the background region from 4 to 7.5 MeV has the greatest effect on producing pileup events in the nitrogen window. A number of large peaks present in the D-T spectrum in this energy region can be seen in Fig. 7. Thus, a lower background continuum, as seen in the D-D pulse height spectrum, would imply a reduction in count pileup due to a reduction in the lower energy events. A quantitative estimate of the effect of these events would require the application of a secondary algorithm to the initial Monte Carlo results, which is beyond the scope of the present article.

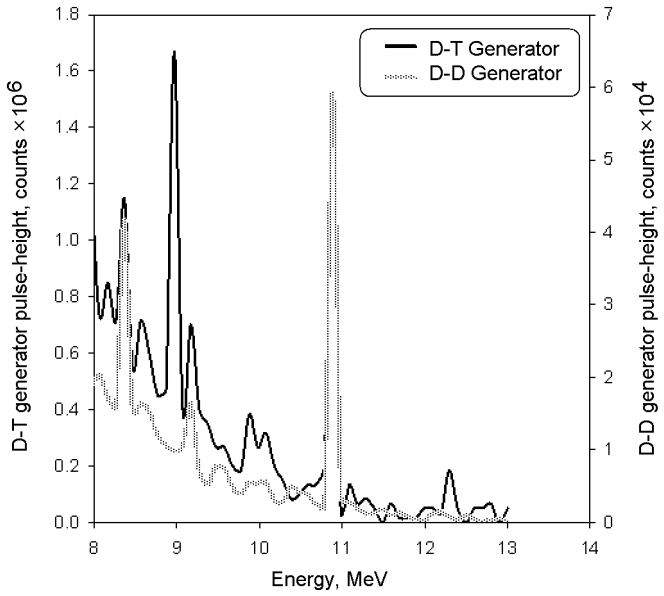

Fig. 6. Pulse-height spectra for photon events produced via neutron activation for two neutron sources

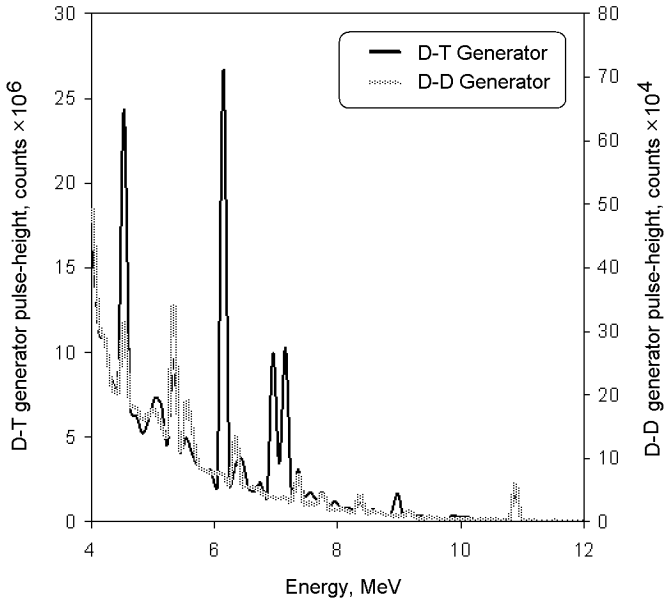

Fig. 7. Pulse-height spectra displaying lower energy events potentially contributing to pulse pileup in nitrogen window

However, we would expect that the D-D spectrum should result in a reduction in background interference. Additionally, when measuring smaller pediatric patients, the production of unwanted gammas by neutrons within the detectors is sharply reduced for the D-D generator, leading to an overall improvement in signal-to-noise ratio.

The benefit of an increased signal attributed to the use of the D-T generator is balanced by interference from the larger background and greater pulse pileup seen with that unit. Its potential advantage, according to the pulse height spectra, may be the greater penetration of its higher energy particles, which would be required when measuring very large subjects (e.g., obesity, edema). In terms of overall efficiency, the D-D generator has a clear advantage, both in pulse height seen in the detectors, and in efficient gamma production within the subject torso. The drawback with our current D-D generator is its low neutron output. Future simulations of the D-D generator operating in a pulsed mode, with gamma detection gated to the thermal neutron region of the pulse, are proposed.

Conclusions

The D-D neutron generator has certain advantages over the D-T generator for the CNRC neutron irradiator facility. These are improved gamma production efficiency, decreased background, both from detector activation and pulse pileup, and lower dose to the subject. However, the low neutron yield available with the present D-D generator does not produce a sufficient nitrogen gamma count rate to warrant its use in studies of adults. Nevertheless, with the D-D generator positioned closer to the scanning bed, it may prove useful in measuring smaller-sized subjects (clinical pediatric population).

*

This work is a publication of the USDA/ARS Children's Nutrition Research Center, Department of Pediatrics, Baylor College of Medicine, and Texas Children's Hospital, Houston, TX. Funding has been provided from the USDA/ARS under Cooperative Agreement No. 58-6250-6-001. The contents of this publication do not necessarily reflect the views or policies of the USDA, nor does mention of trade names, commercial products, or organizations imply endorsement by the US Government.

References

1. R. J. SHYPAILO, K. J. ELLIS, J. Radioanal. Nucl. Chem., 263 (2005) 759.
2. A. H. BEDDOE, A. ZUIDMEER, G. L. HILL, Phys. Med. Biol., 29 (1984) 371.
3. I. E. STAMATELATOS, F. A. DILMANIAN, R. MA, L. J. LIDOFSKY, D. A. WEBER, R. N. PIERSON, Y. KAMEN, S. YASUMURA, Phys. Med. Biol., 38 (1993) 615.
4. R. G. ZAMENHOF, O. L. DEUTSCH, B. W. MURRAY, Med. Phys., 6 (1979) 179.
5. B. J. MCGREGOR, B. J. ALLEN, Australas. Phys. Eng. Sci. Med., 10 (1987) 155.
6. F. A. DILMANIAN, L. J. LIDOFSKY, I. STAMATELATOS, Y. KAMEN, S. YASUMURA, D. VARTSKY, R. N. PIERSON, D. A. WEBER, R. I. MOORE, R. MA, Phys. Med. Biol., 43 (1998) 339.
7. D. VARTSKY, W. V. PRESTWICH, B. J. THOMAS, J. T. DABEK, D. R. CHETTLE, J. H. FREMLIN, K. STAMMERS, J. Radioanal. Chem., 48 (1979) 243.
8. J. F. BRIESMEISTER (Ed.), LA-12625-M, 1997.
9. K. J. ELLIS, R. J. SHYPAILO, H. P. SHENG, W. G. POND, J. Radioanal. Nucl. Chem., 160 (1992) 159.
10. H. HSIAO-HUA, K. J. KEARFOTT, Nucl. Instr. Meth., A422 (1999) 914.
11. A. PAZIRANDEH, M. AZIZI, S. F. MASOUDI, Appl. Radiation Isotopes, 64 (2006) 1.
12. L. A. BAUR, B. J. ALLEN, A. ROSE, N. BLAGOJEVIC, K. J. GASKIN, Phys. Med. Biol., 36 (1991) 1363.
13. C. J. EVANS, S. J. S. RYDE, D. A. HANCOCK, F. AL-AGEL, Appl. Radiation Isotopes, 49 (1998) 541.
14. M. TENHUNEN, J. PYYKKONEN, M. TENHUNEN-ESKELINEN, K. JAATINEN, J. T. KUIKKA, Phys. Med. Biol., 41 (1996) 1209.
15. K. G. MCNEILL, D. J. BOROVNICAR, S. S. KRISHNAN, H. WANG, C. WAANA, J. E. HARRISON, Phys. Med. Biol., 34 (1989) 53.